Arctic sea ice thickness characteristics in winter 2004 and 2007 from submarine sonar transects

Peter Wadhams,[1,2] Nick Hughes,[3] and João Rodrigues[1]

Received 21 January 2011; revised 16 May 2011; accepted 14 June 2011; published 27 September 2011.

[1] A transect of the Arctic Ocean by the British submarine *Tireless* in March 2007 enabled the thickness characteristics of the ice cover to be measured during the winter immediately preceding the exceptional retreat of summer 2007. In this paper we report on mean and modal drafts, probability density functions of draft, and the frequency and depth distribution of pressure ridges, and we compare results with those from an earlier submarine cruise in winter 2004 which covered part of the same area. In the region from north of Fram Strait to Ellesmere Island (about 85°N, 0–70°W) we find no change in mean drafts between 2004 and 2007 though there is a change in ice composition, with more ridging in 2007 but a lesser modal draft. This agrees with the observations of younger ice being driven toward Fram Strait in 2007. The region north of Ellesmere Island continues to be a "redoubt" containing more thick deformed multiyear ice than any other part of the transect. In the west the submarine profiled extensively under the SEDNA ice camp at 73°N 145°W. This is in the same location as the 1976 AIDJEX ice camp and a sonar survey done by a U.S. submarine in April 1976. We found that a large decrease in mean draft had occurred (32%) over 31 years and that in 2007 the SEDNA region contained the thinnest ice of any part of the Arctic surveyed by the submarine; this was a region from which the ice completely retreated during the subsequent summer of 2007.

Citation: Wadhams, P., N. Hughes, and J. Rodrigues (2011), Arctic sea ice thickness characteristics in winter 2004 and 2007 from submarine sonar transects, *J. Geophys. Res.*, *116*, C00E02, doi:10.1029/2011JC006982.

1. Introduction

[2] In summer 2007 the Arctic Ocean experienced an exceptional sea ice retreat, ending with an area that was 1.6 million km^2 less than in any preceding year [*Stroeve et al.*, 2008]. Local field measurements carried out during the summer melt period [*Perovich et al.*, 2008] and model experiments [*Steele et al.*, 2010] both showed that a direct cause of the retreat was in situ melt of the end-of-winter ice cover, mainly from the bottom. To estimate the magnitude of the ice area loss through in situ melt as opposed to transport out of the Basin, it is necessary to know the distribution of ice thickness during the winter preceding the exceptional summer. This information is available from an upward-looking echo sounder survey of the region carried out in March 2007 by HMS *Tireless*. We will show that thickness distributions from the region which became ice-free are such that extensive loss of area could have been expected, while other parts of the Arctic are more resilient because of possessing relatively less thin (i.e., undeformed first-year (FY)) ice.

2. The *Tireless* Voyage

[3] In March 2007 the Royal Navy (RN) sent *Tireless* on a transect of the Arctic Ocean from Fram Strait to the Beaufort Sea, during which she mapped sea ice draft both with conventional upward-looking sonar and with multibeam sonar, the first time that this has been deployed in a submarine. This was the latest in a series of data-gathering cruises using UK submarines that began with HMS *Oracle* [*Wadhams*, 1978b] and *Dreadnought* [*Williams et al.*, 1975] in 1971. The surveys also included voyages by *Sovereign* in 1976 [*Wadhams*, 1978a, 1981], which involved the first use of side scan sonar and a collaboration with an overflying laser-equipped aircraft; and by *Superb* in 1987 [*Wadhams*, 1992; *Wadhams et al.*, 1991; *Comiso et al.*, 1991] which collaborated with aircraft equipped with SAR, laser profilometer and microwave radiometers, flying along identical tracks to the submarine. More recent thickness mapping voyages were by *Trafalgar* in 1996 [*Wadhams and Davis*, 2000, 2001] and *Tireless* in 2004 [*Hughes and Wadhams*, 2006]. For the 2007 *Tireless* cruise we installed a Kongsberg EM3002 multibeam sonar in a sonar dome on the submarine's bow, to supplement the existing single-beam upward sonar system (Admiralty Type 780).

[4] A track chart of the 2004 and 2007 voyages is shown in Figure 1, together with ice limits in summer (16 September)

[1]Department of Applied Mathematics and Theoretical Physics, University of Cambridge, Cambridge, UK.
[2]Laboratoire d'Océanographie de Villefranche, Université Pierre et Marie Curie, Villefranche-sur-Mer, France.
[3]Forecasting Division for Northern Norway, Norwegian Ice Service, Tromsø, Norway.

0148-0227/11/2011JC006982

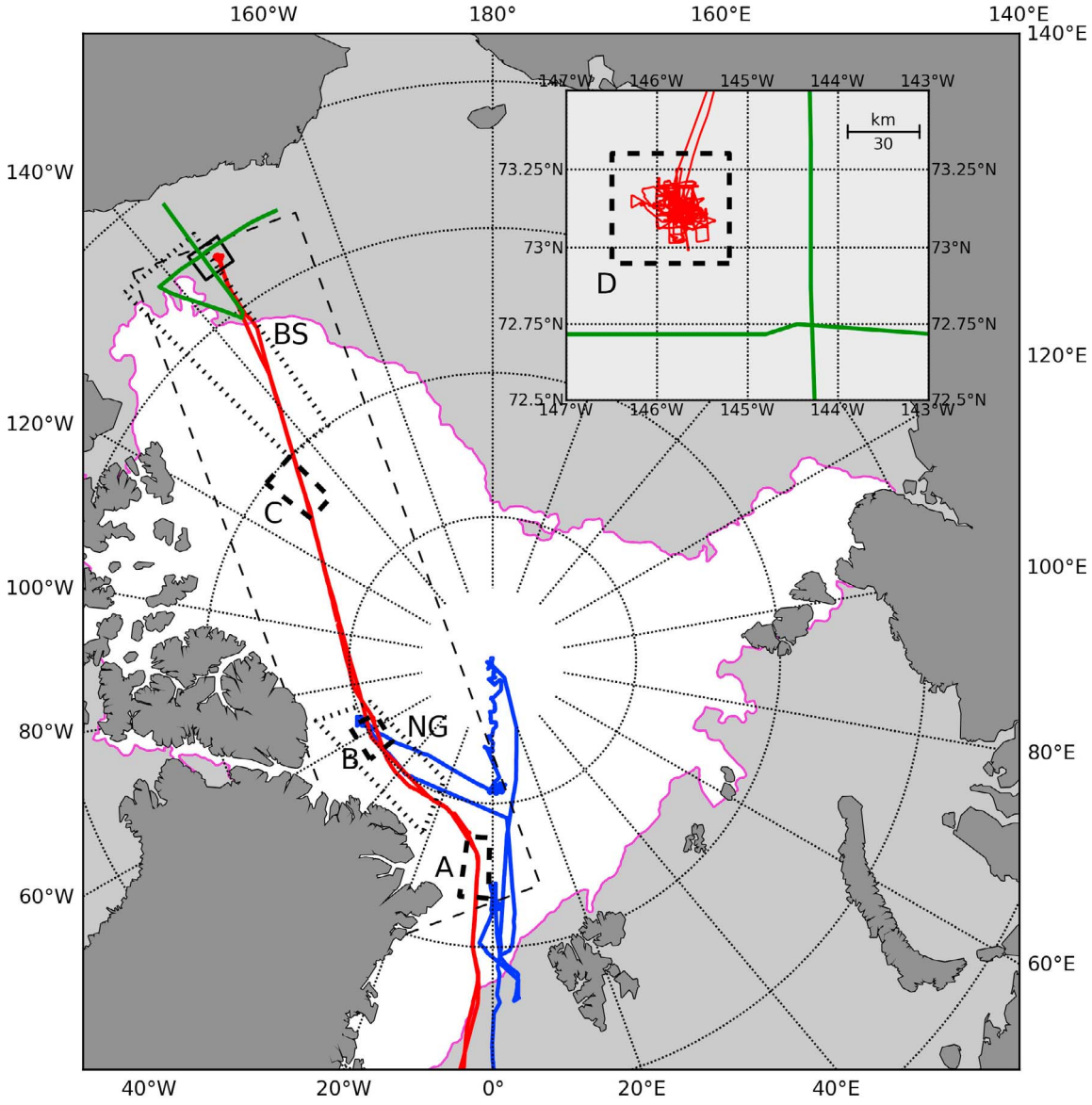

Figure 1. Tracks of the 2004 (blue) and 2007 (red) Tireless voyages compared with the ice extent on 16 September 2007 (from *National Snow and Ice Data Center*, 2007). Inset shows track of the 2007 voyage in the SEDNA ice camp survey, March 14–21, compared with track of USS Gurnard (green) in survey of the AIDJEX ice camp region, April 1976. Letters refer to regions giving data used in Figure 5 (A, B, C, D) and Figure 7 (NG, BS).

2007. The western extremity of the 2007 track surveyed a part of the winter ice cover which later became ice-free. This extremity comprised a special grid survey of the SEDNA (Sea Ice Experiment: Dynamic Nature of the Arctic) [*Hutchings et al.*, 2008] ice camp in the Beaufort Sea in the vicinity of 73°N 145°W. The inset to Figure 1 shows an expanded version of the submarine track during the SEDNA survey, superimposed on a track chart of an ice mapping voyage by USS *Gurnard* carried out in the same area in April 1976 in support of the AIDJEX ice camp [*Wadhams and Horne*, 1980]. The fortunate accident of having two intensive surveys covering essentially identical parts of the ocean, done during the same season but 31 years apart, gives us an opportunity to examine long-term changes in ice morphology during this interval.

[5] An explosion on board *Tireless*, caused by a faulty oxygen generator, occurred in the SEDNA region on March 21, after which the submarine returned to the UK along its outward track. It still collected sonar data, but as it traveled at greater speed and depth the data quality was lower. Data from the return voyage have not been used for the current paper, except in the longitude range 70–100°W where the upward echo sounder was inoperative during the outward voyage.

[6] The earlier 2004 track included a transect to and from the Pole and a diversion to 85°N 62°W in order to survey under a region which a month later was used for an ice camp experiment as part of the EU GreenICE project. This enabled the profiled ice to be studied by drilling, helicopter electromagnetic sounding [*Haas et al.*, 2008], and the use of tiltmeters to

derive thickness from wave dispersion. It was also possible to compare the submarine data with coincident images acquired by the Envisat SAR [*Hughes and Wadhams*, 2006].

[7] Both the 2004 and the 2007 cruise traversed the remaining area or "redoubt" of Arctic multiyear ice north of Greenland and Ellesmere Island. Multiyear ice, formerly the predominant ice type in the Arctic Basin, has shrunk back in recent years to this limited area [*Kwok et al.*, 2009], which has hitherto been inaccessible to ice thickness studies utilizing U.S. submarine data [*Rothrock et al.*, 1999; *Kwok and Rothrock*, 2009] or satellite radar altimetry [*Giles et al.*, 2008]. This is because declassified U.S. submarine data are limited to the "Gore Box" region [*National Science Foundation*, 1998] while radar altimeter satellites available up to 2007 had orbits that limited coverage to latitudes south of 81°30′N. The submarine transects therefore give us a picture of the developing state of the region which contains the largest concentration of old ice in the Basin.

3. Data Analysis

[8] Along-track single-beam upward looking sonar data were recorded using the Admiralty Type 780 echo sounder, which operates at 48 kHz with transducers (fitted on bow, fin and stern) having a nominal 3° beam width. Additionally, the boat in 2004 and 2007 carried a newer Admiralty Type 2077 system, comprising a digitally recording upward sonar coupled both to the submarine inertial navigation system (SINS) and to a pressure transducer. This did not function continuously, so to ensure compatibility of data sets we use only the 780 data here. Other sensors included an upward-looking side scan sonar, an along-track oceanographic sensor package, an expendable bathythermograph (XBT) launcher, an upward-looking video and (in 2007) the multibeam sonar. Results from these sensors will be reported in future papers.

[9] The 780 data were recorded on electrically sensitive paper on a recorder which ran at a constant speed. A one-minute time code provided an indicator of the consistency of recorder speed. To reduce the data to draft versus time, the following steps were necessary: (1) digitization of record (first return from sonar); (2) removal of vertical variation of the waterline representation, due to depth changes and porpoising of the boat; and (3) use of the submarine position to reduce the horizontal time axis to a distance record.

[10] Digitization was carried out on a Kodak scanner using a constant intensity threshold for sonar beam detection. The submarine's positional data were made available at one-second intervals from the SINS and sound velocity was inferred from the along-track oceanographic sensor package and XBTs.

[11] The finite width of the sonar beam introduces a bias in the measurement of the ice draft. The observed draft, taken as the locus of first returns from the sonar, is higher than the real draft by an amount that depends on the beam width, the depth of operation and the roughness of the underside of the ice. As such, it is inappropriate to quantify this bias by a single number. However, estimates for the difference between the mean values of the observed and the real drafts for a certain transect (such as a 50 km section of track) can be obtained from numerical simulation. This is based on the assumption that an accurate ice underside profile can be found (for example from the central beam of a modern multibeam sonar which has a beam width in the along-track direction of less than 1.5°) which can then be convolved by running over it with our wider beam sonar [see, e.g., *Wadhams*, 1981]. These simulations can be carried out for any range of values of the beam width, sensor depth and roughness of the bottom surface of the ice, leading to an empirical relation between the bias and the latter quantities. At typical submarine depths and for the abovementioned nominal beam width we estimate the bias toward thicker ice to be 40–50 cm [*Rodrigues*, 2011]. A second bias, this time toward thinner ice, is introduced during the process of selecting the water level. In many cases water level can be easily identified in the record as a horizontal (or slightly undulating if the submarine is porpoising) homogeneous (structureless) band which is often darker than the rest of the record due to a stronger reflection of the sound wave at the water/air interface than at the water/ice interface. However, it is possible to mistake thin ice (typically up to 30 cm thick) for open water. Hence, we can say that the bias due to errors in the determination of water level is of the order of 15cm, in agreement with *Rothrock and Wensnahan* [2007].

[12] We have not compensated for these possible biases in the analyses presented here, since we are comparing data sets from different years obtained using the same instrument.

4. Results

4.1. Mean and Modal Drafts

[13] A division of the track into 50 km sections produced 64 sections of data from the 2004 cruise and 141 from the 2007 cruise (69 from outgoing portion). It can be seen from Figure 1 that across the north of Greenland, at around 85°N, both cruises followed similar tracks. Satellite data providing coverage of the ice conditions in the area were acquired from the Advanced Synthetic Aperture Radar (ASAR) sensor on the European Space Agency's (ESA's) Envisat satellite, operating in Wide Swath Mode (WSM). This is shown, together with mean drafts from each 50 km section (located at the centroid of the section), in Figure 2. Comparison with data from 1976 and 1987 along similar tracks which cross the north of Greenland [*Wadhams*, 1990] shows a continuing thinning in the region 20°–30°W from mean drafts of 5.5–6.5 m (1976) to 4.5–6.0 m (1987) to 3.5–4.0 m (2004, 2007). This is a highly significant decrease, in line with results from *Rothrock et al.* [1999] drawn from other parts of the Arctic.

[14] Mean drafts averaged 3–4 m from Fram Strait to 30°W in both years, rising to 5–6 m west of 50°W, on entering the well-known zone of heavy ridging and mainly multiyear (MY) ice situated north of Ellesmere Island. This region has been used as the "100% multiyear" tie point for implementations of the NASA Team algorithm for interpreting passive microwave data [*Steffen and Schweiger*, 1991]. It is also a zone where the flow of ice from the Transpolar Drift Stream divides, with some heading east, some west, and some southeast into the Lincoln Sea and Nares Strait. The flow is very variable (as tracked by satellite buoys during the GreenICE and DAMOCLES projects [*Gudmandsen*, 2005]) and allows some ice to remain for many years in the same region, growing thicker and more heavily ridged. This is predicted to be the last redoubt of a reduced MY ice cover if in future summers the Arctic ice

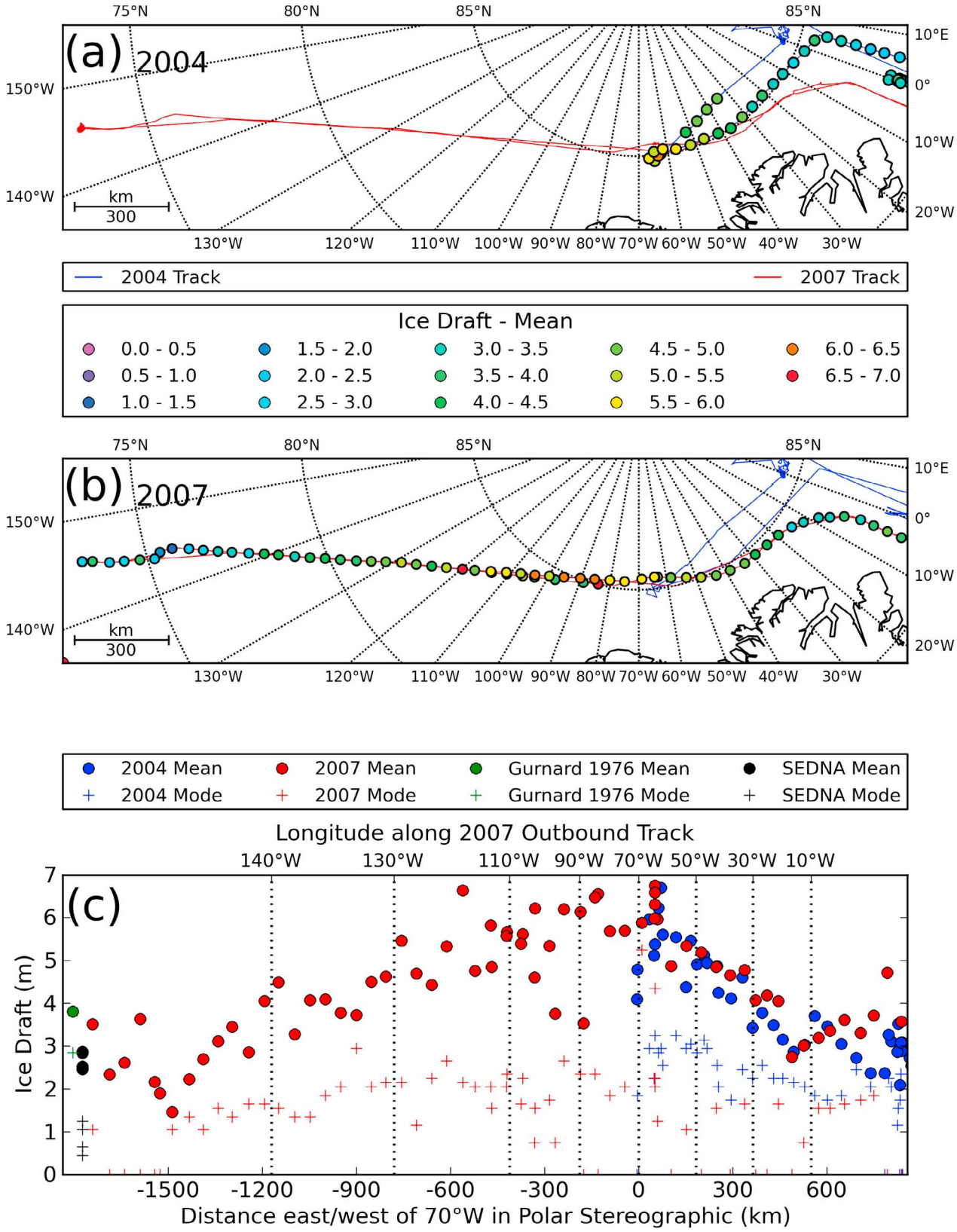

Figure 2. Color-coded mean drafts from 50 km sections of (a) 2004 and (b) 2007 cruises. (c) Mean (solid circles) and modal (crosses) drafts from 50 km sections of the 2004 cruise and 2007 outward tracks, plotted as functions of eastward distance starting from 70°W reference line in a polar stereographic projection is also shown. Black data points are from the SEDNA ice camp region, while green data point is the mean of April 1976 data from same region.

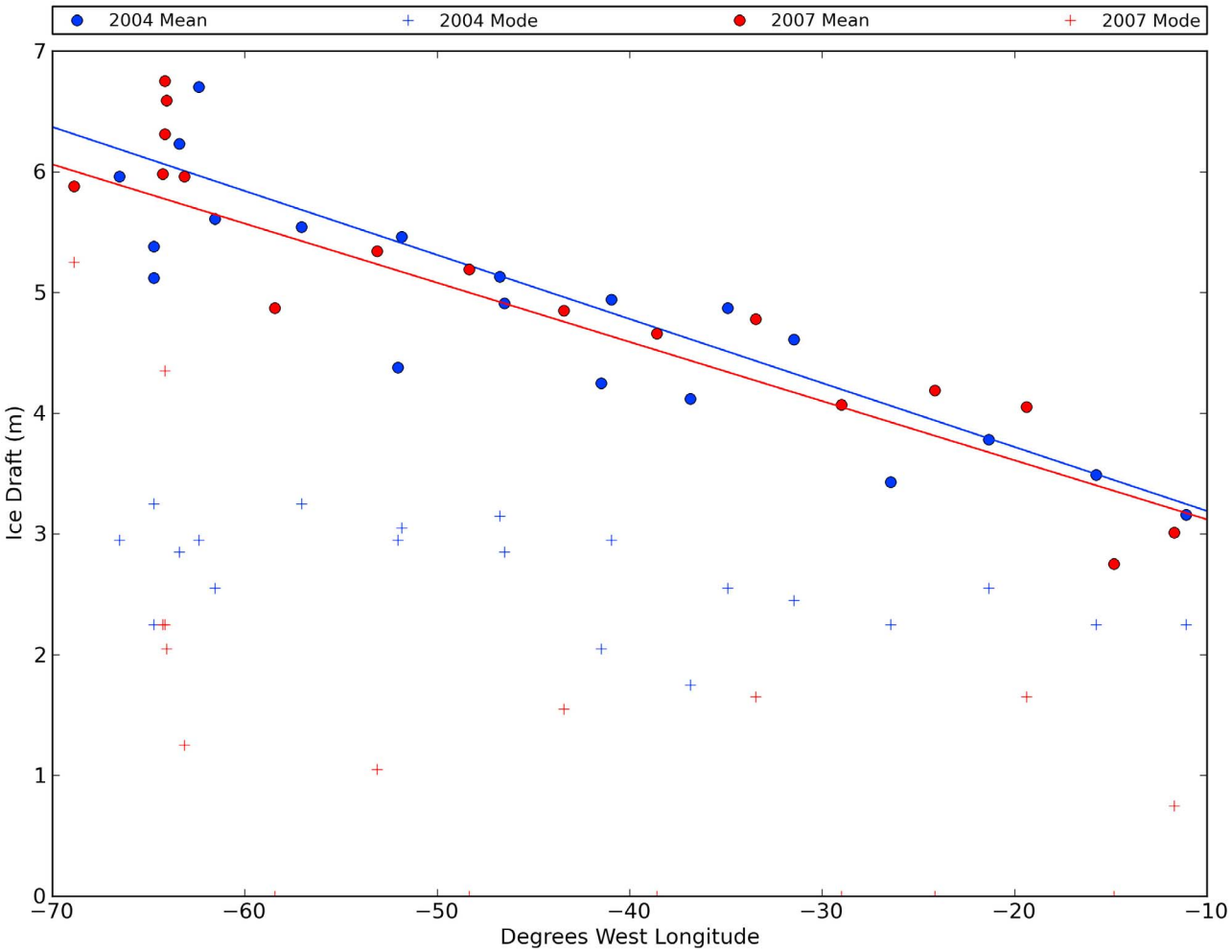

Figure 3. Linear regressions of mean draft versus longitude for the range 10°–70°W in 2004 and 2007, showing almost identical trends.

has substantially melted away [*Nghiem et al.*, 2007]. The highest mean draft in 2004 was 6.70 m at 85°N 63°W, close to the GreenICE site, and in 2007 was 6.75 m in the very similar location of 85°N 64°W. By contrast, ice at the North Pole itself (2004) had a lower mean draft of 4.10 m.

[15] It can be seen from Figure 2 that from about 10°W to 70°W the tracks of the 2004 and 2007 cruises were in close enough coincidence that the data can be directly compared. The lower part of Figure 2 shows plots of mean and modal drafts from 2004 and from the outward voyage of 2007 as a function of eastward distance from a 70°W reference line on a polar stereographic projection. Within the 10° to 70°W zone the geographical change of mean draft can be approximated by a linear regression of draft against longitude (Figure 3), and we see that the best linear fits for 2004 and 2007 are virtually identical:

$$\text{2004 mean draft (m)} = 2.66 + (0.053 \times \text{longitude °W})\ r^2 = 0.90 \quad (1)$$

$$\text{2007 mean draft (m)} = 2.63 + (0.049 \times \text{longitude °W})\ r^2 = 0.82 \quad (2)$$

[16] It is interesting that these similar relationships prevail despite differing ice compositions. We conclude the following: (1) The *spatial pattern* of the mean ice thickness in winter across a wide swath of the Arctic Ocean, from the region north of Ellesmere Island, across the north of Greenland, and into Fram Strait, stayed relatively steady from 2004 to 2007, and mirrored the pattern in earlier years except for significantly lower mean thicknesses. (2) Within the region in which coincident submarine tracks are obtained, there is *no evidence of further thinning* between winter 2004 and winter 2007.

[17] The *modal draft*, also plotted in the lower part of Figure 2, is the draft of the peak of the probability density function (pdf) where the data are allocated to 10 cm bins. Clearly the mode, the most densely populated category of the pdf, corresponds to the thickness achieved by the most common type of thermodynamically grown ice within the 50 km sample, since deformed ice is distributed over many depth categories. It is different for the two years. In 2004 the mode was about 3 m from 40° to 70°W, typical of dominance by MY ice, dropping toward 2 m to the east, again indicative of MY ice that is thinning, possibly due to downstream melt. In 2007 the mode was less than 2 m throughout the 0° to 70°W region. Some values are only 1 m, characteristic of refrozen leads also seen in Figure 2b. The undeformed ice in

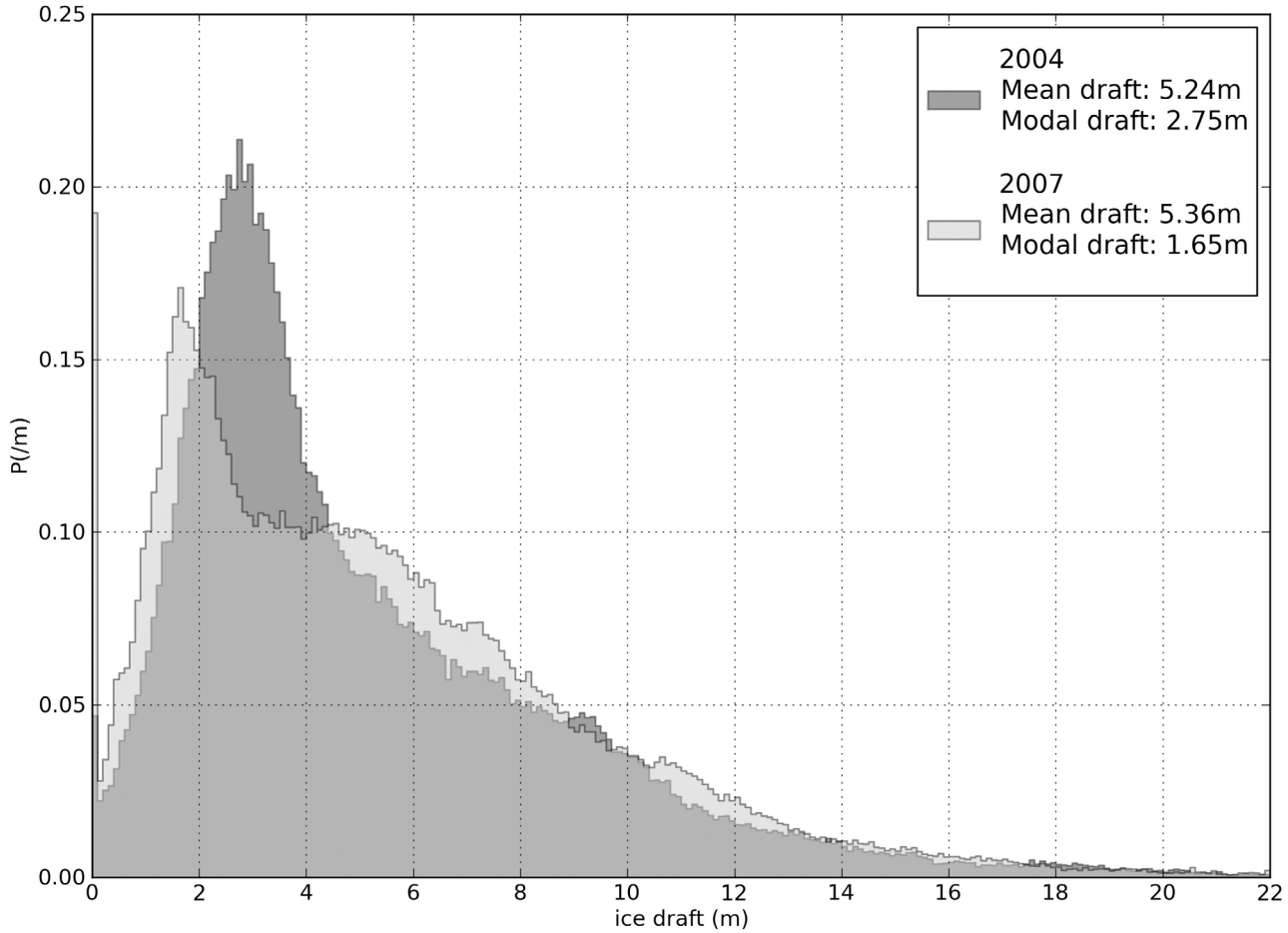

Figure 4. Overall probability density functions for the track sectors between 20°W and 70°W at about 85°N, north of Greenland, for 2004 and 2007 data. Note lower mode in 2007 and greater ridging.

2007 thus tended to be younger and thinner than in 2004, but the ice field was more heavily ridged, giving the same value for the overall mean.

[18] An especially valuable data set was obtained at the western end of the 2007 transect. The mean draft diminishes as the submarine penetrates into the Beaufort Sea, with the minimum at the furthest west. Sections from the SEDNA camp survey area (black in Figure 2c) show this region as having a lower mean draft than any other part of the Arctic Ocean covered by the survey, including the sections within Fram Strait. Uniquely, we have the opportunity for a direct comparison with the data collected in April 1976, 31 years earlier, by USS *Gurnard* [*Wadhams and Horne*, 1980], which carried out a survey of the same limited geographical region, then occupied by the AIDJEX (Arctic Ice Dynamics Joint Experiment) ice camp. This coincidence is due to the fact that ice camps are established by aircraft from Deadhorse or Barrow and so tend to be in the same region. The overall mean draft from 1400 km of data in the 1976 survey area (green circle in Figure 2c) was 3.81 m, while the 2007 SEDNA area mean was 2.58 m, only 68% of the 1976 thickness. This discrepancy would be even greater if we took account of beam width effects in the 2007 survey which would have been greater than with the very narrow-beam instrument used by the 1976 survey. Modes of 2.7–3.0 m, typical of MY ice, occurred in 1976, while the SEDNA modes (1.0–1.3 m) are of FY ice or refrozen leads. This shows that there has been a complete switch in ice character between the two widely separated surveys, a conclusion which is also confirmed by the findings of *Kwok and Rothrock* [2009].

4.2. Distribution of Drafts

[19] Examination of the complete probability density function of ice draft gives greater insight into these changes of ice field character. First we examine our discovery that the patterns of mean ice drafts north of Greenland were similar in 2004 and 2007 despite a radical change in modal drafts. In Figure 4, overall pdfs from 2004 and 2007 for the track sectors from 20°W to 70°W are compared. The significant mode in 2007 was at a depth characteristic of FY ice (1.65 m), even though some contributions by MY ice were clearly present because of the flattening of the pdf in the range 3–5 m before it enters into the exponential tail which characterizes the ridged ice. In 2004 there was a single modal peak, at 2.75 m, which is characteristic of undeformed MY ice, or at very least of second-year ice. However, note that this generally older ice has a tail to its pdf which lies below the tail for 2007 (except for one small protuberance), indicating a lesser contribution from ridging

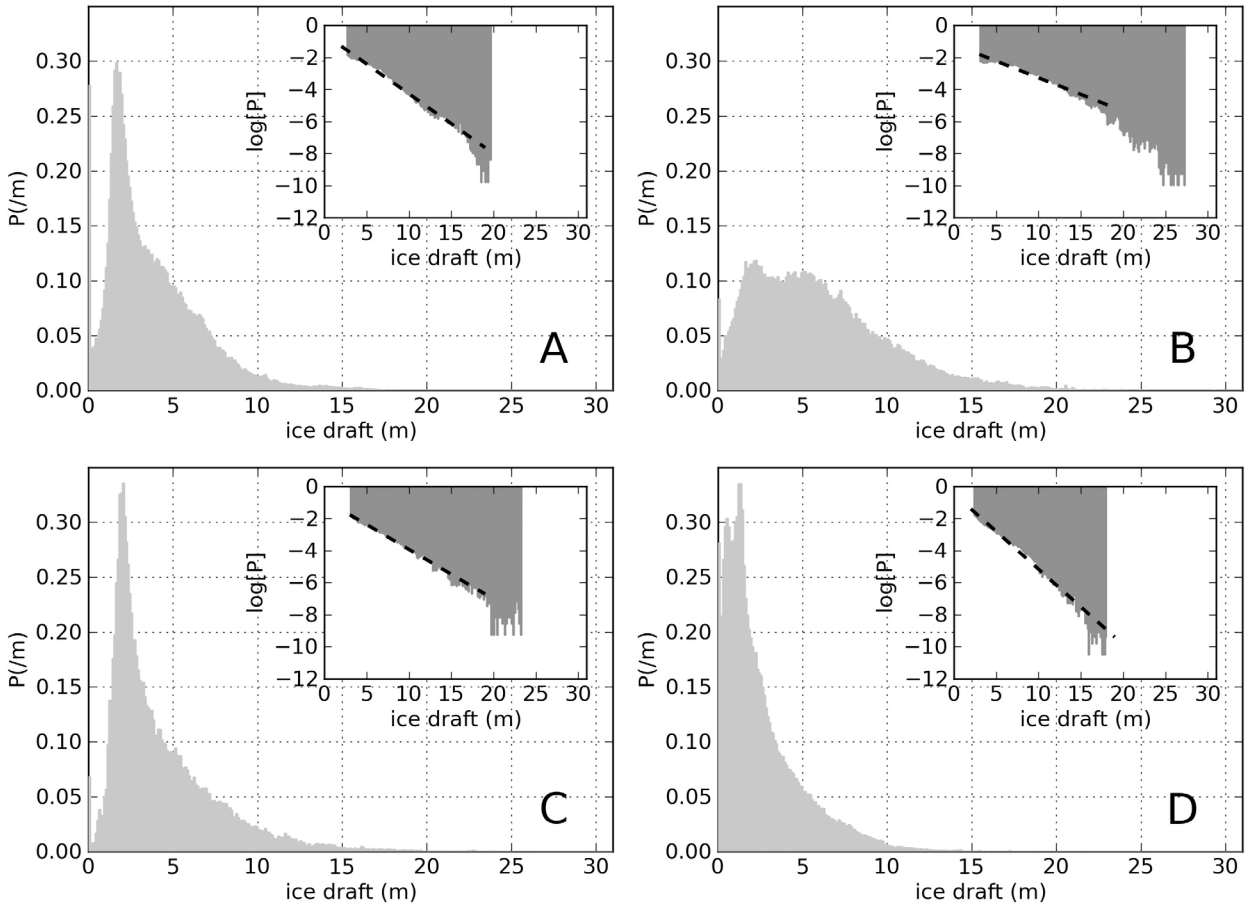

Figure 5. Four typical plots of linear and semilogarithmic pdfs of ice draft from 200 km track sections in four regions of the Arctic, defined in text and shown in Figure 1. Data are plotted in 10 cm bins, and semilog plots show lines of best fit to negative exponential distribution.

in 2004 even though the ice is older and there is apparently no FY present. This is a counter-intuitive exception to the normal rule of thumb, that MY ice fields are more heavily ridged than FY ice fields. We know [*National Snow and Ice Data Center*, 2007] that the 2007 summer minimum corresponded to a heavy ice year in Fram Strait, with buoy trajectories showing a rapid ice drift toward the Strait [*Lindsay et al.*, 2009]. Such a rapid flow opens up the ice cover, producing large areas of refrozen lead (as in Figure 2b), and also new ridging from the differential kinematics. This new ridging, as the floes jostled one another to escape through Fram Strait, is the source of the heavy FY ridging contribution. Thus these results back up the ice dynamics data and support our earlier conclusion for this region: *2004 older ice, less ridging; 2007 younger ice, more ridging*.

[20] We expand our treatment of 2007 pdfs by looking at four regions, concatenating data into 200 km sections to improve resolution and displaying the results in 10 cm bins. Figure 5 is the result, shown as a linear pdf and (insets) on a semi-logarithmic scale with the thinnest categories suppressed. The four regions A, B, C and D are as follows (Table 1).

[21] In Table 1 the "slope" (units m^{-1}) is the parameter β in the relationship P(h)

$$\mathrm{dh} \;=\; \mathrm{A}\exp(-\beta \mathrm{h})\ \mathrm{dh}\ (\mathrm{h} > 5\ \mathrm{m}) \qquad (3)$$

where P(h) is probability density and A is a constant, which has been found to give a good description of the shape of the sea ice draft pdf at drafts which exceed those of undeformed ice [*Wadhams*, 1992, 2000]. The semilogarithmic insets to Figure 5 show that regions A, C and D fit this relationship well. A low slope indicates a relatively large amount of very thick deformed ice, which can be seen to be the case in

Table 1. Four Regions of Arctic Ocean Giving Ice Statistics Shown in Figure 5

Region	Location	Mean (m)	Mode (m)	Slope (m^{-1})
A	Fram Strait: 81.7–83.8°N, 4–8°W	3.79	1.65	0.37
B	N Greenland, Ellesmere: 85°N, 51–65°W	5.92	2.05	0.21
C	NE Beaufort Sea: 80–82°N, 128–135°W	4.40	2.05	0.31
D	SEDNA area: 73°N, 145°W	2.58	1.35	0.47

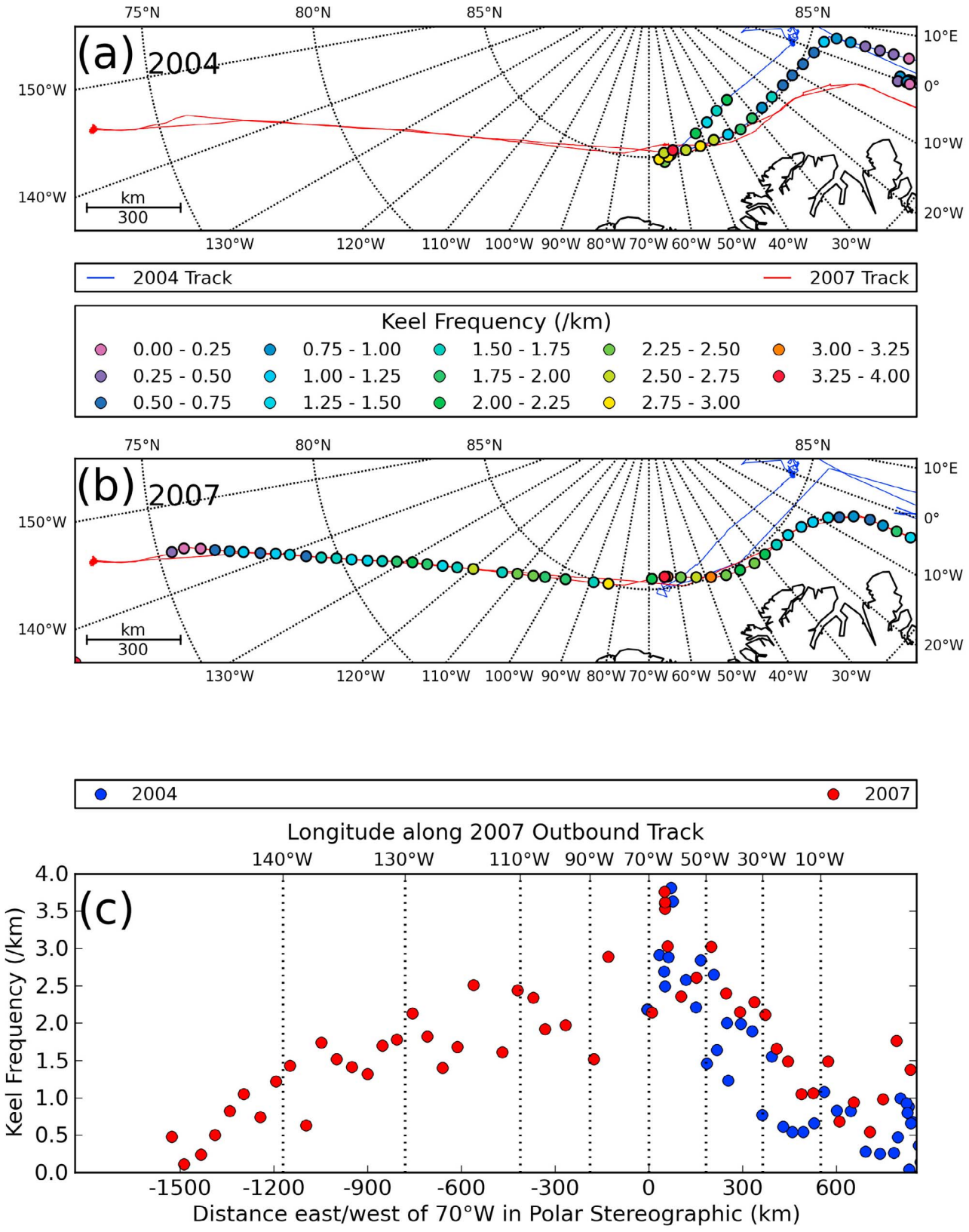

Figure 6. Frequency (km^{-1}) of pressure ridge keels deeper than 9 m in (a) 2004 and (b) 2007. (c) Pressure ridge keel frequencies (>9 m) plotted against distance east of 70°W reference line in polar stereographic projection.

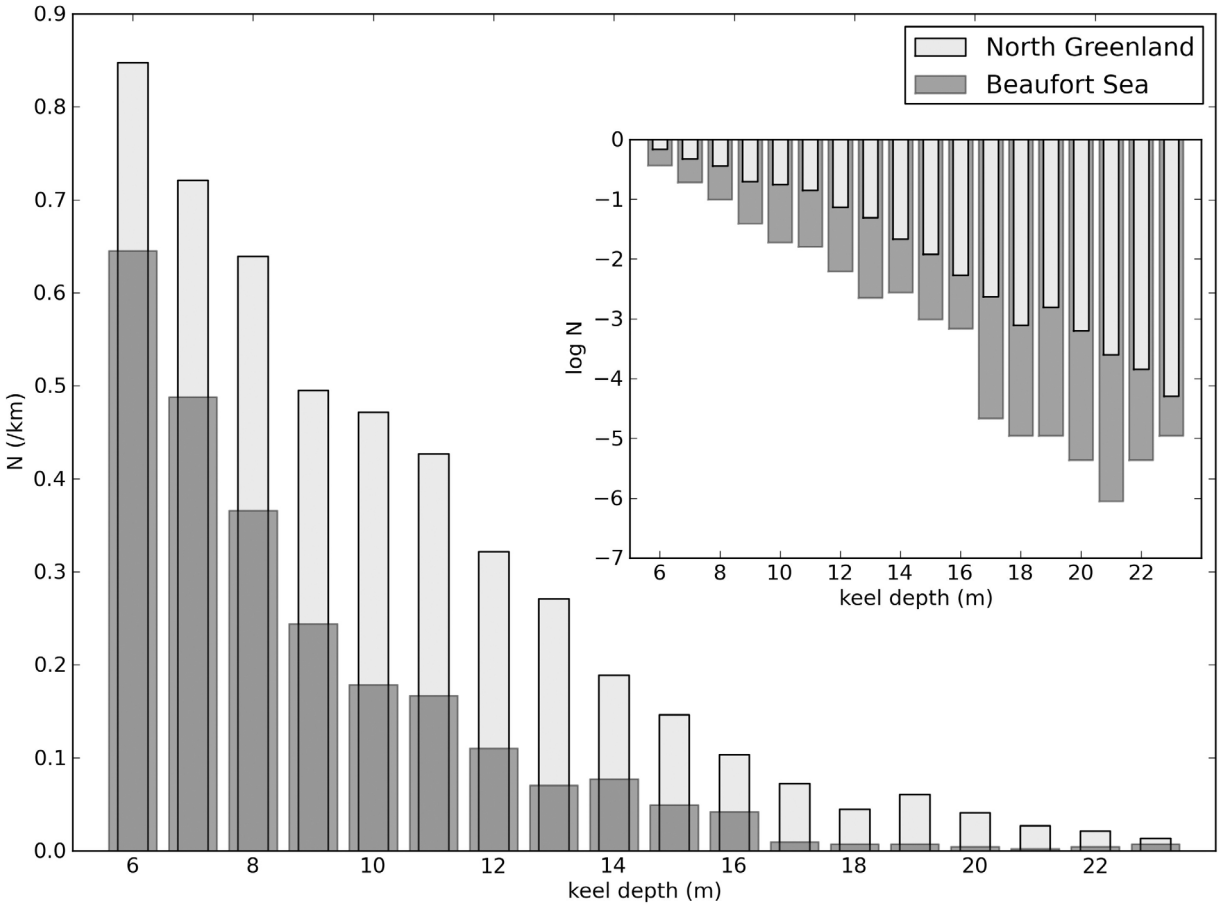

Figure 7. Pressure ridge draft distributions from two contrasting regions: Beaufort Sea (BS), 426 km of data, latitude 75°–80°, longitude 135.5°–145.5°W, mean ice draft 3.35 m; and North Greenland (NG), 516 km of data, latitude 85°, longitude 22°–70°W, mean ice draft 5.35 m. Regions are located on Figure 1. Inset shows ridge frequencies on semilogarithmic scale.

area B, the Ellesmere redoubt, as opposed to the SEDNA area and Fram Strait.

[22] The overall shape of the pdfs in Figure 5, and in particular the location of the modes, reveal the nature of the dominant ice types. Area C is the simplest, with a single sharp mode showing the dominance of a single ice type of undeformed draft 2.0–2.1 m, i.e., thick FY or 2Y ice, and a single negative exponential fitting the ridged ice depth categories. Area D is also simple: the mode is of thinner, definitely FY ice (1.35 m) with a lesser peak at an even lower draft, representing refrozen leads. The ridges fall away in probability more rapidly than area C, demonstrating a relative dearth of deep ridges in the SEDNA area of the Beaufort Sea compared with the NE Beaufort Sea. Area A is mainly composed of FY ice of modal draft 1.65 m, but the inflection in the pdf at 3–5 m draft shows that some MY ice is present, even though the fall-off with increasing depth is still a simple negative exponential. Area B, north of Greenland, is the only region to possess MY ice in comparable quantities to FY ice, as shown by the wide flat peak to the curve extending up to 5 m draft, and the intimate mixture of ice types results in a ridged ice distribution which, alone of the four regions, is not a simple negative exponential as given by equation (3). In fact the slope of the distribution changes from 0.21 (as given in Table 1) at lower drafts to 0.42 at higher drafts of 15–22.5 m (both regression lines are shown on Figure 5).

4.3. Pressure Ridges

[23] Now that multibeam sonar images are available which show the entire shape of a pressure ridge keel, we can study the full 3-dimensional structure of individual ridges. For a comparison with past data sets, however, we here use the 780 data with individual ridges defined as in previous analyses [*Wadhams*, 2000]: an independent ridge is defined as having a crest draft, relative to the local undeformed ice, which is more than double that of the troughs which bracket it. This is based on the Rayleigh criterion in optics and serves as a means (imperfect, but standardized) of separating individual ridges from crest points which are part of a complex ridge.

[24] In terms of numbers of ridges per km of track, Figure 6 compares the density of ridging across the range of longitudes in which the 2007 and 2004 tracks are almost coincident. We focus on ridges deeper than 9 m (implying a sail plus keel thickness exceeding 10 m) and we find from the bottom graph that most sections had more ridges in 2007 than in 2004 in this critical region. By plotting these densities on a map (Figures 6a and 6b) we see that much of the difference can be ascribed to the most heavily ridged region extending further

Table 2a. Ridge Table for 2007

Region	>5 m Keels		>9 m Keels	
	Density (km^{-1})	Mean Draft (m)	Density (km^{-1})	Mean Draft (m)
A	4.25	7.94	1.02	11.8
B	6.13	9.91	3.12	12.75
C	5.22	8.53	1.72	12.4
D	3.84	7.23	0.64	11.16

to the east in 2007 than in 2004, toward the Fram Strait entrance. We recognize the expected similarity between the geographical variations in keel frequencies (Figure 6c) and in mean ice draft (Figure 2c), because of the large contribution that ridges make to the overall mean ice thickness.

[25] It has already been found in a large number of experiments [*Wadhams*, 2000] that the *distribution* of keel drafts in an ice field is a very good fit to a negative exponential distribution, i.e.,

$$n(h)dh = B\exp(-bh)dh, h > h_0 \quad (4)$$

where n(h) is the number of keels per km of track per m of draft increment, and B,b are derived in terms of the experimentally observed mean keel draft (h_m), the mean number of keels per unit distance (n_k) and a low level cutoff draft (h_0):

$$b = (h_m - h_0)^{-1} \quad (5)$$

$$B = n_k b \ \exp(bh_0) \quad (6)$$

[26] *Wadhams and Davy* [1986] confirmed the validity of the negative exponential relationship by a careful examination of keel depths involving the use of order statistics. Figure 7 shows how well this relationship holds for data from the 2007 cruise. It shows data from two regions, one in the Beaufort Sea in the area 75°–80°N, 135.5°–145.5°W, and the other N of Greenland, in the area 85°N, 22°–70°W (locations are marked on Figure 1). As we have already seen from the probability density functions of ice draft, the Beaufort Sea region is almost entirely composed of FY ice while the N Greenland region is a mix of FY and MY ice. In both cases (see inset semilogarithmic plot) the distribution of drafts is a good fit to a negative exponential, while it is apparent that in the region containing MY ice there are more ridges per km in every depth category, and also a lower exponent b in equation (4) showing that deep ridges are relatively more prevalent in the MY than in the FY ice zone.

[27] Table 2a below shows the frequencies and mean drafts of ridges deeper than 5 m and 9 m for the same four regions used in Table 1, while Table 2b compares the ridge statistics for 2004 and 2007 profiles in the common region shown in Figure 3.

[28] From Table 2a we see that the exceptionally high mean ice draft north of Ellesmere Island (region B, Table 1) is directly related to the prevalence of deep ridges, and that over all four areas there is a strong correlation between mean ice draft and ridge frequency. As an exception to this general rule, however, we see from Table 2b that in 2007 there were more ridges per km than in 2004 in the region north of Greenland but with about the same mean draft. The additional contribution of deep ice by ridges in 2007 appears to have been just sufficient to make up for the lesser modal draft of undeformed ice due to the greater prevalence of FY ice in the ice regime

5. Conclusions

[29] Sea ice in the Arctic Ocean has been in retreat since the 1950s [*Berner et al.*, 2005], at a rate of 2.8–4.3% loss of area per decade, measured since 1979 by microwave satellites [*Parkinson et al.*, 1999], which speeded up to 10.7% per decade from 1996 onwards [*Comiso et al.*, 2008]. At the same time, however, submarine sonar measurements have shown that the ice has been thinning much more rapidly, by some 43% in the 25 years between the early 1970s and late 1990s [*Rothrock et al.*, 1999, 2003, 2008; *Wadhams and Davis*, 2000, 2001; *Yu et al.*, 2004] with a loss of ridged ice being especially dramatic (e.g., *Wadhams and Davis* [2001] found only 27% as many ridges 9 m deep or more between Svalbard and the Pole in 1996 relative to 1976).

[30] The thinning rate implies that at some critical date the annual cycle of thickness will have a summer minimum at which a substantial fraction of the winter ice cover will disappear, with the thinner component (mainly undeformed FY ice) melting completely. It is therefore important to know the thickness distribution during the preceding winter. The March 2007 submarine voyage provided this opportunity. We have seen that the ice in the Beaufort Sea, in a region which subsequently became ice-free, was extraordinarily thin, with only 68% of the mean draft of ice in the same region in 1976. Its characteristics indicated that most of the undeformed ice present was FY or refrozen leads, while in the past it was MY. If we examine the Beaufort Sea probability density function, for instance (Figure 4, area D), we find an overall mean draft of 2.58 m and that 43% of the ice cover was less than 2 m thick. The 2 m of melt measured by *Perovich et al.* [2008] during the summer of 2007 would therefore remove 43% of the ice area by melt alone, more than adequate to fragment the rotting ice into disconnected floes and ridge fragments that can easily be swept toward Fram Strait by the prevailing summer wind field.

[31] In the redoubt region north of Greenland and Ellesmere Island at about 85°N 40–80°W, the mean ice thickness was very high, there was little undeformed ice and much of that was MY, and the ice is therefore likely to be the most resistant to rapid basin-wide melt. Comparison with the winter 2004 cruise of the same boat shows that from 70°W to Fram Strait the mean drafts, and their geographical trends, were essentially identical. Even so, the 2007 data showed that the undeformed ice was younger and thinner than in 2004, offset by a greater amount of ridging.

[32] The ability of submarines to obtain probability density functions of ice thickness (as well as ridge shapes) over long distances makes it essential that submarine and/or long-range

Table 2b. Ridge Table for 2004 and 2007 From North Greenland at 85°N, Approximately 20–70°W

Year	>5 m Keels		>9 m Keels	
	Density (km^{-1})	Mean Draft (m)	Density (km^{-1})	Mean Draft (m)
2004	5.50	9.55	2.55	12.72
2007	5.86	9.54	2.72	12.69

AUV missions should continue through this critical period when we see Arctic sea ice changing so rapidly. It is welcome that the U.S. Navy (via the SCICEX program) and the Royal Navy have indicated a continued commitment to Arctic sea ice thickness mapping.

[33] **Acknowledgments.** The authors wish to acknowledge the support of the Office of Naval Research, under grant N00014-07-1-0517; of the UK Ministry of Defense (DSTL); and of the European Union in the DAMOCLES and Arctic Tipping Points projects. The continuing support of the Royal Navy, deployed through the Maritime Warfare Centre, Gosport, is gratefully acknowledged. P.W. and N.H. are grateful to the captain and crew of HMS *Tireless* for their hospitality and supportiveness.

References

Berner, J., et al. (2005), *Arctic Climate Impact Assessment*, 1042 pp., Cambridge Univ. Press, Cambridge, U. K.

Comiso, J. C., P. Wadhams, W. B. Krabill, R. N. Swift, J. P. Crawford, and W. B. Tucker III (1991), Top/bottom multisensor remote sensing of Arctic sea ice, *J. Geophys. Res.*, *96*(C2), 2693–2709, doi:10.1029/90JC02466.

Comiso, J. C., C. L. Parkinson, R. Gersten, and L. Stock (2008), Accelerated decline in the Arctic sea ice cover, *Geophys. Res. Lett.*, *35*, L01703, doi:10.1029/2007GL031972.

Giles, K. A., S. W. Laxon, and A. L. Ridout (2008), Circumpolar thinning of Arctic sea ice following the 2007 record ice extent minimum, *Geophys. Res. Lett.*, *35*, L22502, doi:10.1029/2008GL035710.

Gudmandsen, P. (2005), Lincoln Sea and Nares Strait, in *Proceedings of the 2004 Envisat & ERS Symposium* [CD-ROM], edited by H. Lacoste and L. Ouwehand, Eur. Space Agency, Noordwijk, Netherlands.

Haas, C., A. Pfaffling, S. Hendricks, L. Rabenstein, J.-L. Etienne, and I. Rigor (2008), Reduced ice thickness in Arctic Transpolar Drift favors rapid ice retreat, *Geophys. Res. Lett.*, *35*, L17501, doi:10.1029/2008GL034457.

Hughes, N. E., and P. Wadhams (2006), Measurement of Arctic sea ice thickness by submarine 5 years after SCICEX, *Ann. Glaciol.*, *44*, 200–204, doi:10.3189/172756406781811619.

Hutchings, J., et al. (2008), Role of ice dynamics in the sea ice mass balance, *Eos Trans. AGU*, *89*(50), 515–516, doi:10.1029/2008EO500003.

Kwok, R., and D. A. Rothrock (2009), Decline in Arctic sea ice thickness from submarine and ICESat records: 1958–2008, *Geophys. Res. Lett.*, *36*, L15501, doi:10.1029/2009GL039035.

Kwok, R., G. F. Cunningham, M. Wensnahan, I. Rigor, H. J. Zwally, and D. Yi (2009), Thinning and volume loss of the Arctic Ocean sea ice cover: 2003–2008, *J. Geophys. Res.*, *114*, C07005, doi:10.1029/2009JC005312.

Lindsay, R. W., J. Zhang, A. Schweiger, M. Steele, and H. Stern (2009), Arctic sea ice retreat in 2007 follows thinning trend, *J. Clim.*, *22*, 165–176, doi:10.1175/2008JCLI2521.1.

National Science Foundation (1998), Newly Declassified Submarine Data Will Help Study of Arctic Ice, *Press Release 98-006*, Arlington, Va. [Available at http://www.nsf.gov/news/news_images.jsp?cntn_id = 102863&org = NSF.]

National Snow and Ice Data Center (2007), Arctic sea ice shatters all previous record lows: Diminished summer sea ice leads to opening of the fabled Northwest Passage, press release, Boulder, Colo. [Available at http://www.nsidc.org/news/press/2007_seaiceminimum/20071001_pressrelease.html.]

Nghiem, S. V., I. G. Rigor, D. K. Perovich, P. Clemente-Colón, J. W. Weatherly, and G. Neumann (2007), Rapid reduction of Arctic perennial sea ice, *Geophys. Res. Lett.*, *34*, L19504, doi:10.1029/2007GL031138.

Parkinson, C. L., D. J. Cavalieri, P. Gloersen, H. J. Zwally, and J. C. Comiso (1999), Arctic sea ice extents, areas, and trends, 1978–1996, *J. Geophys. Res.*, *104*(C9), 20,837–20,856, doi:10.1029/1999JC900082.

Perovich, D. K., J. A. Richter-Menge, K. F. Jones, and B. Light (2008), Sunlight, water and ice: Extreme Arctic sea ice melt during the summer of 2007, *Geophys. Res. Lett.*, *35*, L11501, doi:10.1029/2008GL034007.

Rodrigues, J. (2011), Beamwidth effects on sea ice draft measurement from UK submarines, *Cold Reg. Sci. Technol.*, *65*(2), 160–171, doi:10.1016/j.coldregions.2010.09.005.

Rothrock, D. A., and M. Wensnahan (2007), The accuracy of sea ice drafts measured from US Navy submarines, *J. Atmos. Oceanic Technol.*, *24*(11), 1936–1949, doi:10.1175/JTECH2097.1.

Rothrock, D. A., Y. Yu, and G. A. Maykut (1999), Thinning of the Arctic sea-ice cover, *Geophys. Res. Lett.*, *26*(23), 3469–3472, doi:10.1029/1999GL010863.

Rothrock, D. A., J. Zhang, and Y. Yu (2003), The arctic ice thickness anomaly of the 1990s: A consistent view from observations and models, *J. Geophys. Res.*, *108*(C3), 3083, doi:10.1029/2001JC001208.

Rothrock, D. A., D. B. Percival, and M. Wensnahan (2008), The decline in arctic sea-ice thickness: Separating the spatial, annual, and interannual variability in a quarter century of submarine data, *J. Geophys. Res.*, *113*, C05003, doi:10.1029/2007JC004252.

Steele, M., J. Zhang, and W. Ermold (2010), Mechanism of summertime upper Arctic Ocean warming and the effect on sea ice melt, *J. Geophys. Res.*, *115*, C11004, doi:10.1029/2009JC005849.

Steffen, K., and A. Schweiger (1991), NASA Team Algorithm for sea ice concentration retrieval from Defense Meteorological Satellite Program Special Sensor Microwave Imager: Comparison with Landsat satellite imagery, *J. Geophys. Res.*, *96*(C12), 21,971–21,987, doi:10.1029/91JC02334.

Stroeve, J., et al. (2008), Arctic sea ice extent plummets in 2007, *Eos Trans. AGU*, *89*(2), 13–14, doi:10.1029/2008EO020001.

Wadhams, P. (1978a), Sidescan sonar imagery of sea ice in the Arctic Ocean, *Can. J. Rem. Sens.*, *4*(2), 161–173.

Wadhams, P. (1978b), Wave decay in the marginal ice zone measured from a submarine, *Deep-Sea Res.*, *25*, 23–40.

Wadhams, P. (1981), Sea-ice topography of the Arctic Ocean in the region 70°W to 25°E, *Philos. Trans. R. Soc. London, Ser. A*, *302*, 45–85, doi:10.1098/rsta.1981.0157.

Wadhams, P. (1990), Evidence for thinning of the Arctic ice cover north of Greenland, *Nature*, *345*, 795–797, doi:10.1038/345795a0.

Wadhams, P. (1992), Sea ice thickness distribution in the Greenland Sea and Eurasian Basin, May 1987, *J. Geophys. Res.*, *97*(C4), 5331–5348, doi:10.1029/91JC03137.

Wadhams, P. (2000), *Ice in the Ocean*, 368 pp., Gordon and Breach, London.

Wadhams, P., and N. R. Davis (2000), Further evidence of ice thinning in the Arctic Ocean, *Geophys. Res. Lett.*, *27*(24), 3973–3975, doi:10.1029/2000GL011802.

Wadhams, P., and N. R. Davis (2001), Arctic sea-ice morphological characteristics in summer 1996, *Ann. Glaciol.*, *33*, 165–170, doi:10.3189/172756401781818969.

Wadhams, P., and T. Davy (1986), On the spacing and draft distributions for pressure ridge keels, *J. Geophys. Res.*, *91*(C9), 10,697–10,708, doi:10.1029/JC091iC09p10697.

Wadhams, P., and R. J. Horne (1980), An analysis of ice profiles obtained by submarine sonar in the Beaufort Sea, *J. Glaciol.*, *25*, 401–424.

Wadhams, P., N. R. Davis, J. C. Comiso, R. Kutz, J. Crawford, G. Jackson, W. Krabill, C. B. Sear, R. Swift, and W. B. Tucker (1991), Concurrent remote sensing of Arctic sea ice from submarine and aircraft, *Int. J. Remote Sens.*, *12*, 1829–1840, doi:10.1080/01431169108955212.

Williams, E., C. Swithinbank, and G. d. Q. Robin, (1975), A submarine sonar study of Arctic pack ice, *J. Glaciol.*, *15*(73), 349–362.

Yu, Y., G. A. Maykut, and D. A. Rothrock (2004), Changes in the thickness distribution of Arctic sea ice between 1958–1970 and 1993–1997, *J. Geophys. Res.*, *109*, C08004, doi:10.1029/2003JC001982.

N. Hughes, Forecasting Division for Northern Norway, Norwegian Ice Service, Kirkgårdsveien 60, Tromsø NO-9293, Norway.

J. Rodrigues and P. Wadhams, Department of Applied Mathematics and Theoretical Physics, University of Cambridge, Wilberforce Road, Cambridge CB3 0WA, UK. (p.wadhams@damtp.cam.ac.uk)